



Cite this: *RSC Adv.*, 2019, 9, 31241

Received 8th September 2019  
 Accepted 9th September 2019

DOI: 10.1039/c9ra07203a

[rsc.li/rsc-advances](http://rsc.li/rsc-advances)

# Fe<sup>II</sup>-catalysed insertion reaction of $\alpha$ -diazocarbonyls into X–H bonds (X = Si, S, N, and O) in dimethyl carbonate as a suitable solvent alternative†

Nour Tanbouza,<sup>ID</sup> Hoda Keipour<sup>ID</sup> and Thierry Ollevier<sup>ID</sup>\*

The insertion reaction of a broad range of diazo compounds into Si–H bonds was found to be efficiently catalysed by Fe(OTf)<sub>2</sub> in an emerging green solvent *i.e.* dimethyl carbonate (DMC). The  $\alpha$ -silylated products were obtained in good to excellent yields (up to 95%). Kinetic studies showed that the extrusion of N<sub>2</sub> to form an iron carbene intermediate is rate-limiting. The iron-catalysed insertion reaction of methyl  $\alpha$ -phenyl- $\alpha$ -diazoacetate into polar X–H bonds (S–H, N–H, and O–H) was also established in DMC.

Dimethyl carbonate (DMC), the simplest among the dialkyl carbonate family (DACs), is an emerging and interesting green reagent and solvent alternative in organic synthesis due to its high biodegradability and low toxicity.<sup>1,2</sup> It is exploited industrially for its efficiency as a solvent for numerous applications,<sup>3</sup> however it still remains underused as a solvent in homogeneous catalysis. Even though major contributions have been achieved to promote the twelve principles of green chemistry,<sup>4</sup> searching for efficient green solvent alternatives still remains a challenge for chemists.<sup>5</sup> Solvent selection guides are huge influencers for rendering the choice of an appropriate solvent less tedious in terms of life cycle evaluation.<sup>6</sup>

For this study, we were successful in establishing dimethyl carbonate as an appropriate solvent for an iron-catalysed insertion reaction of acceptor/donor diazo compounds into Si–H bonds and polar X–H bonds (X = S, N, and O). Diazo compounds are the most commonly used carbene precursors. They can be de-diazonized to obtain highly reactive free carbene intermediates or metal carbene species. Then, varieties of chemical transformations can occur, such as X–H (X = C, S, N, O, and Si) insertions,<sup>7</sup> cyclopropanation,<sup>7b</sup> ylide formation,<sup>8</sup> and Wolff rearrangement.<sup>9,10</sup> Notably, the transition metal-catalysed insertion reaction of diazo compounds into various X–H bonds represents a facile route towards different tailored functionalized compounds which are arduous to obtain through other routes.<sup>11</sup>

Special attention has been paid to the insertion reaction of diazo compounds into Si–H bonds, because even though silicon is vastly abundant on earth, routes towards organosilicons are

not. Organosilicon compounds are increasingly mainstream within a variety of applications.<sup>12</sup> They are pertinent in the pharmaceutical sector where the integration of silicon motifs as carbon isosteres has allowed distinctive therapeutic potential in a number of biologically active molecules.<sup>13</sup> The transition metal-catalysed insertion reaction into Si–H bonds is a facile and atom-economic method to produce organosilicons.<sup>14</sup> This reaction was first described by Kramer and Wright in 1963.<sup>15</sup> Since then, pivotal breakthroughs have been made with Ru,<sup>16</sup> Rh,<sup>17</sup> Ir,<sup>18</sup> Ag,<sup>19</sup> Cu,<sup>20</sup> and enzyme-catalysed<sup>21</sup> insertion reactions of diazo compounds into the Si–H bond. Iron catalysis being one of our group's major areas of research,<sup>22</sup> we developed a highly efficient iron-catalysed insertion reaction of  $\alpha$ -diazoesters into Si–H bonds.<sup>23</sup> Afterwards, an enantioselective iron-catalysed version was developed by Xie and Lin.<sup>24</sup> The use of iron salts in transition metal catalysis is gaining traction due to their low toxicity, abundance, and environmental benignity. Iron catalysts have proved on and on to be efficient and green substitutes of conventional noble metal catalysts.<sup>25</sup>

Even though iron-catalysed Si–H insertion reactions were successfully developed to render it more sustainable, they were still conducted in dichloromethane (CH<sub>2</sub>Cl<sub>2</sub>), a solvent which is commonly used in homogeneous catalysis due to its good solubility of most organics, low polarity, and non-coordinating properties. However, it is notorious for its toxicity, harmfulness to both human health and the environment, and costly disposal.<sup>26</sup> Herein, we disclose the use of DMC as an appropriate solvent alternative to CH<sub>2</sub>Cl<sub>2</sub> in a ferrous system for the insertion reaction of  $\alpha$ -diazocarbonyl compounds into Si–H bonds. Kinetic studies are then employed to establish the rate determining step of an iron-catalysed insertion of  $\alpha$ -diazoesters into Si–H bonds. This study is then further extended to cover insertion reactions of  $\alpha$ -diazoesters into different polar X–H bonds (X = O, N, and S).

Département de Chimie, Université Laval, 1045 Avenue de la Médecine, Québec, QC, G1V 0A6, Canada

† Electronic supplementary information (ESI) available: Experimental procedures and copies of <sup>1</sup>H NMR, <sup>13</sup>C NMR, and <sup>19</sup>F NMR spectra. See DOI: 10.1039/c9ra07203a



A series of Fe<sup>II</sup> and Fe<sup>III</sup> salts were selected for screening in DMC with Et<sub>3</sub>SiH (Table 1).<sup>27</sup> The following screening shows that the nature of the catalyst greatly influences the reactivity of the diazo compound. Fe(OTf)<sub>2</sub> was capable of affording the  $\alpha$ -silylated product **2a** in a 95% yield within 6 h (entry 1).<sup>28</sup> FeBr<sub>2</sub> and FeCl<sub>2</sub> led to poor conversions after 72 h (entries 2 and 3). The diazo compound **1a** was unreactive towards Fe(OAc)<sub>2</sub> and was recovered quantitatively (entry 4). Fe(BF<sub>4</sub>)<sub>2</sub>·6H<sub>2</sub>O resulted in a low 6% yield which was due to insertion with H<sub>2</sub>O and dimerization (entry 5). Interestingly, both Fe(OTf)<sub>3</sub> and Fe(acac)<sub>3</sub> led to the formation of the silyl enolate, which was attributed to the strong Lewis acidity of Fe<sup>III</sup> salts (entries 6 and 7).

In order to conduct an appropriate screening of solvents, and to figure out the correlation between the solvent's solvatochromic properties and how it affects the course of this reaction, a Kamlet–Taft plot of aprotic solvents was used to this advantage (Fig. 1).<sup>29</sup> The plot includes different common organic solvents previously screened for this reaction in addition to a screening of different classical and less common green solvent alternatives (see ESI† for individual yields and reaction times). Solvents that produced very good yields of the insertion product (>90%) are coloured green (■), whilst those leading to moderate yields (between 90% and 50%) and poor yields (<50%) are identified in yellow (▲) and red (◆), respectively. As it can be seen from the distribution of solvents on the Kamlet–Taft plot, solvents with high basicity ( $\beta > 0.4$ ) and low polarizability ( $\pi^* < 0.5$ ) resulted in moderate and low yields of the desired insertion product. It can be deduced that the reaction prefers a reaction media that is low in polarity and basicity which is delivered by all of CH<sub>2</sub>Cl<sub>2</sub>, dichloroethane (DCE, (CH<sub>2</sub>Cl)<sub>2</sub>), benzene (PhH), chlorobenzene (PhCl), bromobenzene (PhBr), and DMC. An exception is observed with toluene (PhMe) which is reactive towards metal carbenes. Another is with MeCN; this can be attributed to the low solubility of the silane. Following the solvent selection guides, DMC was chosen for this reaction. Other organic carbonates, *i.e.* diethyl carbonate (DEC) and

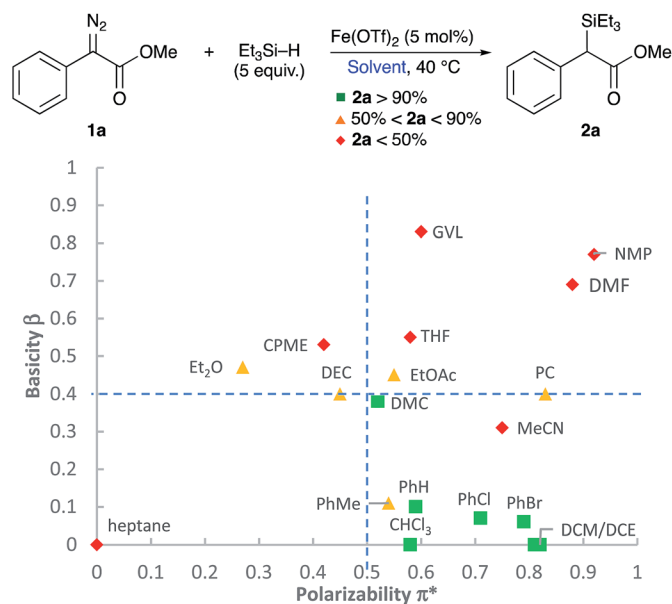


Fig. 1 Kamlet–Taft plot of screened aprotic solvents. Reaction conditions: **1a** (0.25 mmol), Fe(OTf)<sub>2</sub> (5 mol%), Et<sub>3</sub>SiH (1.25 mmol), solvent (2 ml).

propylene carbonate (PC), were not as efficient as dimethyl carbonate. Polar protic solvents, H<sub>2</sub>O and EtOH, were also tested in this reaction where no sign of the insertion product was observed, and only O–H insertion products were obtained in high yields (see ESI†).

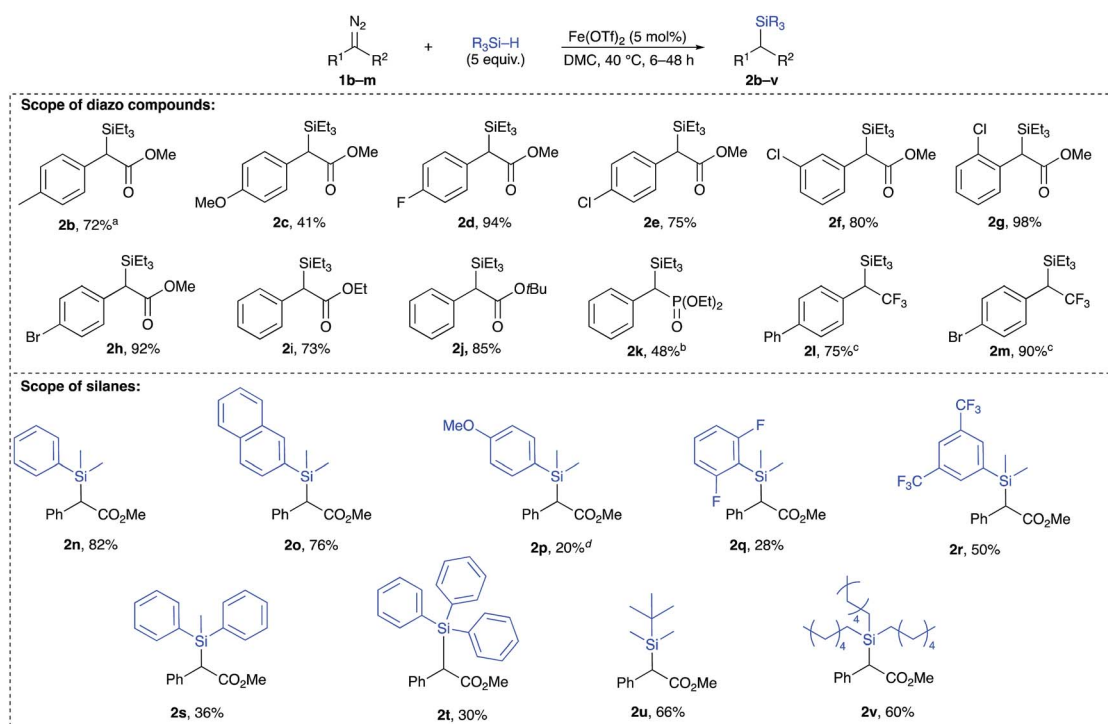
A broad range of acceptor/donor  $\alpha$ -diazo compounds and silanes was examined to demonstrate the tolerance of this catalytic system (Table 2). Electron-donating groups in the *p*-position of the aryl group were tolerated as seen for cases **2b** and **2c**. Also,  $\alpha$ -diazoesters with electron-withdrawing groups in the *o*-, *p*-, and *m*-positions of the aromatic ring (**2d–h**) allowed the reaction to proceed with good to excellent yields. Different ester functionalities were found to be well-tolerated (**2i–k**). Interestingly, the  $\alpha$ -diazophosphonate **1l** underwent complete conversion after 72 h to yield 48% of the corresponding insertion product **2l**. The diazotrifluoromethyl substrates **1m** and **1n** efficiently underwent the insertion reaction to give rise to the  $\alpha$ -silylated products in 75% and 90% yields, respectively. The Si–H insertion reaction of methyl  $\alpha$ -phenyl- $\alpha$ -diazoacetate **1a** was then conducted with different silanes. An insertion with PhMe<sub>2</sub>SiH led to an 82% yield of **2o** with completion in 12 h. The reaction of the  $\alpha$ -diazoester **1a** with (2-naphthyl)Me<sub>2</sub>SiH achieved completion in 6 h with the corresponding product **2p** in 76%. When tuning the aryl group of an ArMe<sub>2</sub>SiH series, it was observed that a *p*-OMe substituent resulted in an extended reaction time of 24 h with the corresponding silylated product in a 20% yield. An (*o,o'*-F)<sub>2</sub>C<sub>6</sub>H<sub>3</sub> substituted silane produced the insertion product **2r** in 28%. A (*m,m'*-CF<sub>3</sub>)<sub>2</sub>C<sub>6</sub>H<sub>3</sub> substituted silane resulted in a moderate yield (50% of **2s**) with completion in 6 h. Bulkier silanes, such as Ph<sub>2</sub>MeSiH and Ph<sub>3</sub>SiH, were tougher to insert where yields dramatically dropped to 36% and 30%, respectively, in addition to extended reaction times (up to 48 h). For alkyl silanes, the

Table 1 Screening of different metal salts for the insertion of methyl  $\alpha$ -phenyl- $\alpha$ -diazoacetate into Si–H bonds<sup>a</sup>

Entry	MX <sub>n</sub>	Time (h)	Yield (%)
1	Fe(OTf) <sub>2</sub>	6	95
2	FeBr <sub>2</sub>	72	4 <sup>b</sup>
3	FeCl <sub>2</sub>	72	45 <sup>b</sup>
4	Fe(OAc) <sub>2</sub>	48	0 <sup>c</sup>
5	Fe(BF <sub>4</sub> ) <sub>2</sub> ·6H <sub>2</sub> O	18	6 <sup>d</sup>
6	Fe(OTf) <sub>3</sub>	48	— <sup>e</sup>
7	Fe(acac) <sub>3</sub>	48	— <sup>e</sup>

<sup>a</sup> **1a** (0.25 mmol), catalyst (5 mol%), Et<sub>3</sub>SiH (1.25 mmol), DMC (2 ml).  
<sup>b</sup> Incomplete conversion. <sup>c</sup> No conversion and recovery of  $\alpha$ -diazoester **1a**. <sup>d</sup> Insertion with H<sub>2</sub>O and dimerization as major pathways. <sup>e</sup> A mixture of *O*-silyl enolate and dimerization product was obtained.



Table 2 Screening of various acceptor/donor diazo compounds and silanes for the insertion reaction into Si–H bonds<sup>a</sup>

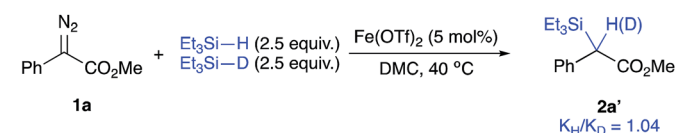
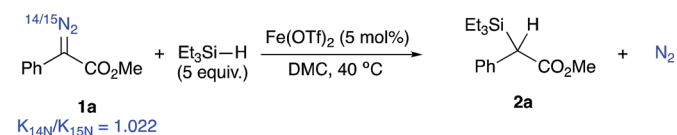
<sup>a</sup> Reaction conditions: diazo compound (0.25 mmol), Fe(OTf)<sub>2</sub> (5 mol%), silane (1.25 mmol), DMC (2 ml), individual reaction time (see ESI). <sup>b</sup> 10 equiv. of Et<sub>3</sub>SiH were used. <sup>c</sup> 25 mg of 4 Å MS were used. <sup>d</sup> Reaction was conducted at rt. <sup>e</sup> Yield calculated by <sup>1</sup>H NMR.

reaction of methyl  $\alpha$ -phenyl- $\alpha$ -diazoacetate with (*t*-Bu)Me<sub>2</sub>SiH and (Hex)<sub>3</sub>SiH afforded the insertion products **2v** and **2w** in moderate yields (66% and 60%, respectively) previous attempts to establish the rate-determining step of an iron catalysed Si–H insertion reaction have been inconclusive.<sup>23,24</sup> Unlike Si–H insertions with other metal catalysts, no H/D kinetic isotope effect was observed after conducting a competition experiment with a D-silane. The competition experiment between Et<sub>3</sub>Si–H and Et<sub>3</sub>Si–D was run again (Fig. 2, eqn (1)), but this time in DMC, using equimolar amounts of both silanes under the previously established optimum conditions. This experiment did not show any sign that the activation of the Si–H bond is rate-determining, where a value of 1.04 was obtained. Thus, we hypothesized that the extrusion of nitrogen to form the iron carbene is most likely the rate-determining step and that the activation of Si–H bond occurs quickly after the formation of the metal carbene.

So, the kinetics of this reaction were placed under scrutiny in order to validate the hypothesis of a rate-determining step governed by the formation of the iron carbene species. In a study by Wu, a nitrogen kinetic isotope effect showed that the formation of a Rh carbene is rate-limiting for a Si–H insertion (Fig. 2, eqn (2)).<sup>31</sup> Such a study was done by using isotope ratio mass spectrometry (IRMS) for the determination of a nitrogen kinetic isotope effect at natural abundance. The ratio of <sup>14</sup>N/<sup>15</sup>N resulting from the natural <sup>15</sup>N-enrichment of unreacted  $\alpha$ -diazoester **1a** during the progression of the insertion reaction was measured by IRMS. This ratio can be used to calculate the kinetic isotope effect from enrichment in the heavy isotope in

a substrate.<sup>32</sup> Given the fact that the extrusion of N<sub>2</sub> is irreversible and that it is not involved in any subsequent step, the measured nitrogen ratios are only relevant to the carbene formation step.

Eq. 1: H/D kinetic isotope effect experiment

Eq. 2: <sup>14</sup>N/<sup>15</sup>N kinetic isotope effect experiment

Eq. 3: Determination of the reaction order

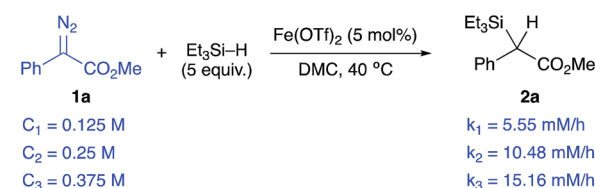


Fig. 2 Kinetic studies for the determination of the rate-limiting step.

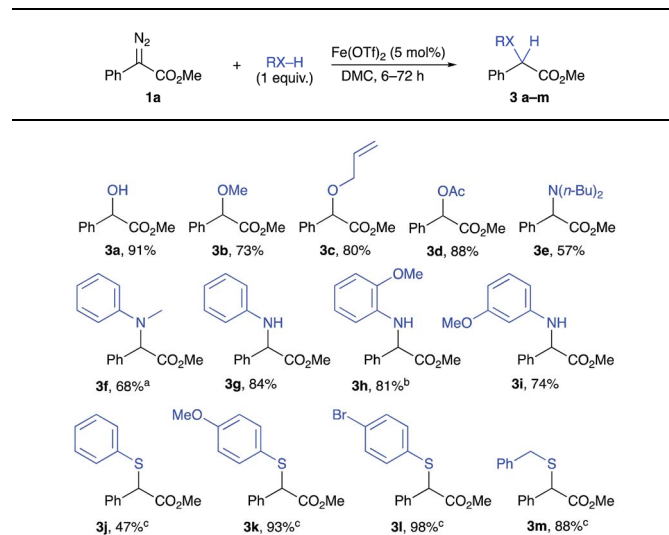


Here, a large and normal heavy KIE value of  $1.022 \pm 0.007$  was obtained, which supports the hypothesis that the formation of the iron carbene intermediate is rate-determining.<sup>33</sup> Also, the insertion reaction was run under pseudo-first order conditions under the optimum conditions with different concentrations of the  $\alpha$ -diaoester **1a** (Fig. 2, eqn (3)). The formation of **2a** was monitored by GC analysis and initial rates were found to be first-order with regard to the concentration of methyl  $\alpha$ -phenyl- $\alpha$ -diaoacetate **1a**. A linear variation was observed between the initial rate and the concentration of **1a**, with  $[1a] = 0.125, 0.25,$  and  $0.5$  M, resulted in initial rates of  $5.55, 10.48,$  and  $15.16$  mM  $h^{-1}$ , respectively. Such results are in accordance with those obtained from a study of an iron-catalysed insertion reaction of diazo compounds into C–H bonds.<sup>34</sup>

With these results in hand, a mechanism can be therefore drawn where the coordination of the diazo species to the iron centre enriches it thus allowing  $\pi$ -back bonding to extrude nitrogen gas (I, Fig. 3). The formation of the Fe carbene II is rate-determining which subsequently reacts with the activated silane in a one-step manner to yield the insertion product **2a** and regenerate the iron catalyst. An alternative mechanism involving the coordination of the terminal nitrogen to the metal centre has thus been refuted.<sup>35</sup>

Polar X–H insertion reactions of methyl  $\alpha$ -phenyl- $\alpha$ -diaoacetate **1a** was then examined (Table 3). Insertions into O–H bonds were conducted in DMC where alcohol **3a** and ethers **3b** and **3c** were obtained in very good yields with completion in 6 h.<sup>36</sup> HOAc has been tested for O–H insertion and proceeds to give the corresponding ester **3d** in an 88% yield. N–H insertions, however, were strongly dependent on the nature of the amine used. Secondary amines **3e** and **3f** were afforded in moderate yields of 57% and 68%, respectively, with prolonged reaction times (72 h) and even required increased temperatures (80 °C) to achieve completion. Improved yields were obtained with primary aromatic amines, where an insertion with aniline led to

Table 3 Polar X–H (X = O, N, and S) insertion reactions with methyl  $\alpha$ -phenyl- $\alpha$ -diaoacetate<sup>a</sup>



<sup>a</sup> Reaction conditions: methyl  $\alpha$ -phenyl- $\alpha$ -diaoacetate (0.25 mmol),  $Fe(OTf)_2$  (5 mol%), X–H (0.25 mmol), DMC (2 ml). <sup>b</sup> 5 equiv. of the amine were used and reaction was conducted at 80 °C. <sup>c</sup> The reaction was concentrated to 0.5 M. <sup>d</sup> 4 equiv. of the thiol and 25 mg of 4 Å MS were used at 80 °C.

the corresponding product **3g** in 84% yield but completion could only be reached after 72 h. Also, when using *o*-anisidine and *m*-anisidine, corresponding amines were obtained in 81% and 74%, respectively (Table 3, **3h** and **3i**). It is important to mention that in all of the three cases using primary amines, the reaction was selective toward a mono-insertion with no sign of a double insertion product. S–H insertions were mediated by an excess of the aryl thiol substrate and using 4 Å MS as an additive along with heating to reflux of DMC. The insertion reaction with thiophenol proceeded in a modest yield of 47% (Table 3, **3j**). A higher yield was obtained when employing a *p*-OMe or a *p*-Br substituted thiophenol affording the corresponding products **3k** and **3l** in 93% and 98%, respectively. The reaction of **2a** with benzyl thiol resulted in **3m** in an 88% yield.

In conclusion, we have successfully realized an iron-catalysed insertion reaction of  $\alpha$ -diao compounds into X–H bonds in DMC as a suitable solvent alternative. A wide range of  $\alpha$ -silylesters were obtained in good to excellent yields. The mechanism of the insertion reaction into Si–H bonds was studied while showing that the formation of the iron carbene intermediate is rate-limiting. This work demonstrates the efficiency of iron carbenes used in insertion reactions and also shows that chlorinated solvents can be advantageously replaced by greener alternatives in diazo chemistry. Further developments in the use of iron carbenes will be reported in due course.

## Conflicts of interest

There are no conflicts to declare.

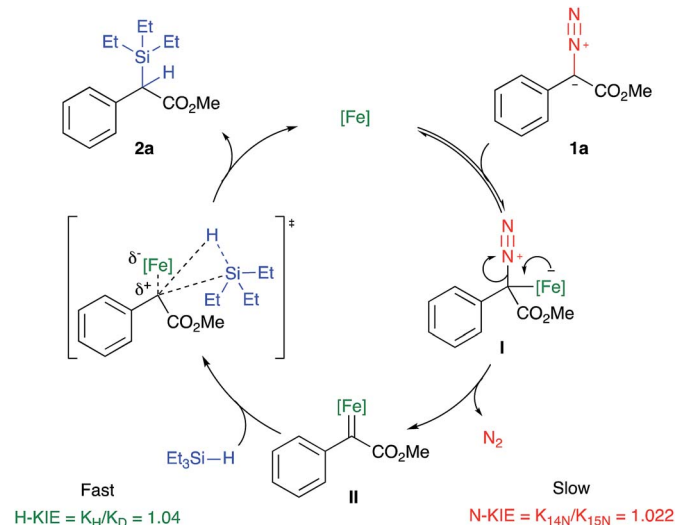


Fig. 3 Plausible mechanism for the iron-catalysed insertion reaction of methyl  $\alpha$ -phenyl- $\alpha$ -diaoacetate into Si–H bonds.



## Acknowledgements

This work was supported by the Natural Sciences and Engineering Research Council of Canada (NSERC) Discovery Grant RGPIN-2017-04272, the FRQNT Centre in Green Chemistry and Catalysis (CGCC) Strategic Cluster FRQNT-2020-RS4-265155-CCVC, and Université Laval. N. T. thanks the Francis & Geneviève Melançon Foundation for a graduate scholarship. H. K. thanks CGCC for a graduate scholarship. We thank Jonathan Gagnon (Laboratoire d'Océanographie, Université Laval) for IRMS measurements.

## Notes and references

- (a) F. Arico and P. Tundo, *Russ. Chem. Rev.*, 2010, **79**, 479–489; (b) B. Schaffner, F. Schaffner, S. P. Verevkin and A. Borner, *Chem. Rev.*, 2010, **110**, 4554–4581.
- (a) U. Romano, F. Rivetti and N. D. Muzio, Italy Pat., 3045767, 1981; (b) P. Tundo, M. Musolino and F. Arico, *Green Chem.*, 2017, **20**, 28–85; (c) A. Li, Y. Pu, F. Li, J. Luo, N. Zhao and F. Xiao, *J. CO<sub>2</sub> Util.*, 2017, **19**, 33–39; (d) Z. Zhang, S. Liu, L. Zhang, S. Yin, G. Yang and B. Han, *Chem. Commun.*, 2018, **54**, 4410–4412.
- (a) A. Sasidharanpillai, C. H. Kim, C. H. Lee, M. T. Sebastian and H. T. Kim, *ACS Sustainable Chem. Eng.*, 2018, **6**, 6849–6855; (b) J. Kraïem, D. Ghedira and T. Ollevier, *Green Chem.*, 2016, **18**, 4859–4864; (c) P. Arockiam, V. Poirier, C. Fischmeister, C. Bruneau and P. H. Dixneuf, *Green Chem.*, 2009, **11**, 1871–1875; (d) X. Miao, C. Fischmeister, C. Bruneau and P. H. Dixneuf, *ChemSusChem*, 2008, **1**, 813–816.
- (a) P. Anastas and N. Eghbali, *Chem. Soc. Rev.*, 2010, **39**, 301–312; (b) H. C. Erythropel, J. B. Zimmerman, T. M. de Winter, L. Petitjean, F. Melnikov, C. H. Lam, A. W. Lounsbury, K. E. Mellor, N. Z. Janković, Q. Tu, L. N. Pincus, M. M. Falinski, W. Shi, P. Coish, D. L. Plata and P. T. Anastas, *Green Chem.*, 2018, **20**, 1929–1961.
- P. G. Jessop, *Green Chem.*, 2011, **13**, 1391–1398.
- (a) A. Jordan and H. F. Sneddon, *Green Chem.*, 2019, **21**, 1900–1906; (b) D. Prat, A. Wells, J. Hayler, H. Sneddon, C. R. McElroy, S. Abou-Shehada and P. J. Dunn, *Green Chem.*, 2016, **18**, 288–296; (c) V. Isoni, L. L. Wong, H. H. Khoo, I. Halim and P. Sharratt, *Green Chem.*, 2016, **18**, 6564–6572; (d) D. Prat, J. Hayler and A. Wells, *Green Chem.*, 2014, **16**, 4546–4551.
- (a) S.-F. Zhu and Q.-L. Zhou, *Acc. Chem. Res.*, 2012, **45**, 1365–1377; (b) G. T. Gurmessa and G. S. Singh, *Res. Chem. Intermed.*, 2017, **43**, 6447–6504.
- H. M. L. Davies, in *Comprehensive Asymmetric Catalysis, Supplement 1*, ed. E. N. Jacobson, A. Pfaltz and H. Yamamoto, Springer, Heidelberg, Germany, 2004. pp. 83–94.
- W. Kirmse, *Eur. J. Org. Chem.*, 2002, 2193–2256.
- (a) M. P. Doyle, *Chem. Rev.*, 1986, **86**, 919–940; (b) T. Ye and M. A. McKervey, *Chem. Rev.*, 1994, **94**, 1091–1160.
- (a) I. Fleming, A. Barbero and D. Walter, *Chem. Rev.*, 1997, **97**, 2063–2192; (b) K. A. Mix, J. E. Lomax and R. T. Raines, *J. Am. Chem. Soc.*, 2017, **139**, 14396–14398; (c) J. Wu and J. S. Panek, *J. Org. Chem.*, 2011, **76**, 9900–9918; (d) D. Gillingham and N. Fei, *Chem. Soc. Rev.*, 2013, **42**, 4918–4931; (e) H. Daorui, C. Shenxin, Z. Xueyan, Y. Qiuhan, Y. Qizheng and D. Zhenya, *Austin J. Anal. Pharm. Chem.*, 2016, **3**, 1–4.
- (a) H. Yang, A. M. Swartz, H. J. Park, P. Srivastava, K. Ellis-Guardiola, D. M. Upp, G. Lee, K. Belsare, Y. Gu, C. Zhang, R. E. Moellering and J. C. Lewis, *Nat. Chem.*, 2018, **10**, 318–324; (b) B. Minkovich, I. Ruderfer, A. Kaushansky, D. Bravo-Zhivotovskii and Y. Apeloig, *Angew. Chem., Int. Ed.*, 2018, **57**, 13261–13265; (c) I. Fleming, A. Barbero and D. Walter, *Chem. Rev.*, 1997, **97**, 2063–2192.
- (a) A. K. Franz and S. O. Wilson, *J. Med. Chem.*, 2013, **56**, 388–405; (b) J. Wu and J. S. Panek, *J. Org. Chem.*, 2011, **76**, 9900–9918.
- H. Keipour, V. Carreras and T. Ollevier, *Org. Biomol. Chem.*, 2017, **15**, 5441–5456.
- K. A. W. Kramer and A. N. Wright, *J. Chem. Soc.*, 1963, 3604–3608.
- Y. Nakagawa, S. Chanthamath, I. Fujisawa, K. Shibatomi and S. Iwasa, *Chem. Commun.*, 2017, **53**, 3753–3756.
- (a) R. T. Buck, M. P. Doyle, M. J. Drysdale, L. Ferris, D. C. Forbes, D. Haigh, C. J. Moody, N. D. Pearson and Q.-L. Zhou, *Tetrahedron Lett.*, 1996, **37**, 7631–7634; (b) Y. Landais and D. Planchenault, *Tetrahedron Lett.*, 1994, **35**, 4565–4568; (c) Y. Landais, L. Parra-Rapado, D. Planchenault and V. Weber, *Tetrahedron Lett.*, 1997, **38**, 229–232.
- Y. Yasutomi, H. Suematsu and T. Katsuki, *J. Am. Chem. Soc.*, 2010, **132**, 4510–4511.
- (a) M. J. Iglesias, M. C. Nicasio, A. Caballero and P. J. Perez, *Dalton Trans.*, 2013, **42**, 1191–1195; (b) Z. Liu, Q. Li, Y. Yang and X. Bi, *Chem. Commun.*, 2017, **53**, 2503–2506.
- (a) L. A. Dakin, P. C. Ong, J. S. Panek, R. J. Staples and P. Stavropoulos, *Organometallics*, 2000, **19**, 2896–2908; (b) Y.-Z. Zhang, S.-F. Zhu, L.-X. Wang and Q.-L. Zhou, *Angew. Chem., Int. Ed.*, 2008, **47**, 8496–8498; (c) H. Keipour, A. Jalba, L. Delage-Laurin and T. Ollevier, *J. Org. Chem.*, 2017, **82**, 3000–3010.
- (a) S. B. Kan, R. D. Lewis, K. Chen and F. H. Arnold, *Science*, 2016, **354**, 1048–1051; (b) F. H. Arnold, *Angew. Chem., Int. Ed.*, 2018, **57**, 4143–4148.
- (a) M. Li, V. Carreras, A. Jalba and T. Ollevier, *Org. Lett.*, 2018, **20**, 995–998; (b) S. Lauzon, H. Keipour, V. Gandon and T. Ollevier, *Org. Lett.*, 2017, **19**, 6324–6327; (c) W. Xu, T. Ollevier and F. Kleitz, *ACS Catal.*, 2018, **8**, 1932–1944.
- H. Keipour and T. Ollevier, *Org. Lett.*, 2017, **19**, 5736–5739.
- H. Gu, Z. Han, H. Xie and X. Lin, *Org. Lett.*, 2018, **20**, 6544–6549.
- (a) I. Bauer and H.-J. Knoelker, *Chem. Rev.*, 2015, **115**, 3170–3387; (b) S.-F. Zhu and Q.-L. Zhou, *Natl. Sci. Rev.*, 2014, **1**, 580–603; (c) K. Gopalaiah, *Chem. Rev.*, 2013, **113**, 3248–3296; (d) H. Keipour, A. Jalba, N. Tanbouza, V. Carreras and T. Ollevier, *Org. Biomol. Chem.*, 2019, **17**, 3098–3102; (e) A. Röske, I. Alt and B. Plietker, *ChemCatChem*, 2019, DOI: 10.1002/cctc.201900459.



- 26 (a) P. M. Schlosser, A. S. Bale, C. F. Gibbons, A. Wilkins and G. S. Cooper, *Environ. Health Perspect.*, 2015, **123**, 114–119; (b) R. Hossaini, M. P. Chipperfield, S. A. Montzka, A. A. Leeson, S. S. Dhomse and J. A. Pyle, *Nat. Commun.*, 2017, **8**, 15962.
- 27 5 equiv. of the silane were required to achieve better yields. However, the remaining silane could be recovered after purification.
- 28 In a control experiment involving Ph<sub>2</sub>MeSiH (1 equiv.) in the presence of the iron catalyst Fe(OTf)<sub>2</sub> (5 mol%) in DMC (2 ml) at 40 °C for 24 h, the silane was found intact and completely recovered. This shows that there is no reaction occurring between the silane and DMC.
- 29 P. G. Jessop, D. A. Jessop, D. Fu and L. Phan, *Green Chem.*, 2012, **14**, 1245–1259.
- 30 Diazo compounds **1l** and **1m** decompose at 40 °C.
- 31 F. M. Wong, J. Wang, A. C. Hengge and W. Wu, *Org. Lett.*, 2007, **9**, 1663–1665.
- 32 R. G. Duggleby and D. B. Northrop, *Bioorg. Chem.*, 1989, **17**, 177–193.
- 33 (a) M. Gomez-Gallego and M. A. Sierra, *Chem. Rev.*, 2011, **111**, 4857–4963; (b) Y. Zhang, J. Bommuswamy and M. L. Sinnott, *J. Am. Chem. Soc.*, 1994, **116**, 7557–7563; (c) S. Jankowski, L. D. Quin, P. Paneth and M. H. O'Leary, *J. Am. Chem. Soc.*, 1994, **116**, 11675–11677; (d) T. Holm, *J. Am. Chem. Soc.*, 1994, **116**, 8803.
- 34 H. M. Mbuvi and L. K. Woo, *Organometallics*, 2008, **27**, 637–645.
- 35 The mechanism is similar to that obtained with a Rh catalyst. See ref. 31.
- 36 Phenol was tested as a substrate for O–H insertion with diazo compound **1a** where the crude showed complex mixtures with the corresponding ether in low yields (19%).

